



## Improving the energy yield of plasma-based NO<sub>x</sub> synthesis with *in situ* adsorption†

Kevin Hendrik Reindert Rouwenhorst,<sup>id</sup>abc Sybe Tabak<sup>a</sup> and Leon Lefferts<sup>id</sup>\*a

Cite this: *React. Chem. Eng.*, 2024, 9, 528

Received 6th November 2023,  
Accepted 17th January 2024

DOI: 10.1039/d3re00593c

rsc.li/reaction-engineering

**Plasma-based NO<sub>x</sub> synthesis from air is a promising option to electrify nitrogen fixation. However, the energy efficiency of direct plasma-based NO<sub>x</sub> synthesis in a plasma reactor is severely limited by NO<sub>x</sub> decomposition in the plasma phase. *In situ* NO<sub>x</sub> adsorption on MgO improves the NO<sub>x</sub> energy yield in a dielectric barrier discharge (DBD) plasma reactor by a factor of 15.**

Plasma-based nitrogen fixation *via* NO<sub>x</sub> synthesis from air was commercialized in the early 20th century. Kristian Birkeland and Samuel Eyde commercialized the first industrial nitrogen fixation process, the Birkeland–Eyde process, based on an electric arc plasma reactor.<sup>1,2</sup> This process was operational in Norway and Canada.<sup>3,4</sup> However, the process was eventually outcompeted by the Haber–Bosch process, producing ammonia (NH<sub>3</sub>) from nitrogen (N<sub>2</sub>) and hydrogen (H<sub>2</sub>) derived from steam reforming of hydrocarbons or from water electrolysis.

Plasma-based nitrogen fixation has re-emerged in scientific literature as an option to electrify N<sub>2</sub> fixation.<sup>5–9</sup> Plasma-based processes have the advantage that the load can be varied quickly, in contrast to thermal processes, so that rapid changes in supply of renewable electricity can be handled.<sup>10</sup> Also, absence of the need for intensive energy integration makes local production at relatively small scale feasible. In particular, plasma-N<sub>2</sub> fixation in the form of NO<sub>x</sub> shows promise.<sup>5,6</sup>

So far, plasma-based NO<sub>x</sub> synthesis in warm plasma reactors such as gliding arc (GA) and microwave (MW) plasma reactors, shows the best performance,<sup>5,6</sup> with NO<sub>x</sub> formation at an energy cost down to 0.42 MJ per mol NO<sub>x</sub>,<sup>11</sup> which is competitive with the renewable Haber–Bosch process (using electrolysis to produce H<sub>2</sub>) combined with the Ostwald process (NH<sub>3</sub> oxidation) in terms of energy cost (0.6 MJ per mol HNO<sub>3</sub>).<sup>6</sup> However, such low energy consumptions for plasma reactors are only achieved when operating at low NO<sub>x</sub> concentrations of typically a few hundred ppm,<sup>11</sup> which is not practical for NO<sub>x</sub> absorption in water in an industrial process.<sup>12</sup> Concentrations in the order of 5 mol% NO<sub>x</sub> are required for efficient processing. For those conditions, the energy consumption for NO<sub>x</sub> formation in plasma reactors is at least in the order of 2 MJ per mol NO<sub>x</sub>.<sup>6</sup> Furthermore, the high temperatures in warm plasmas in the order of 10<sup>3</sup> K cause thermal NO<sub>x</sub> decomposition<sup>13</sup> and rapid quenching is required to minimize thermal NO<sub>x</sub> decomposition.

This work introduces a novel concept for energy-efficient NO<sub>x</sub> formation in a dielectric barrier discharge (DBD) reactor *via in situ* NO<sub>x</sub> removal using a solid MgO sorbent. A DBD reactor is a non-thermal plasma reactor operating near room temperature.<sup>14</sup> Only a few studies have been done using DBD reactors for NO<sub>x</sub> synthesis,<sup>13,15–18</sup> reporting relatively high energy consumption compared to warm plasma reactors. Nevertheless, a DBD reactor has been used in this work for two reasons. Firstly, thermal NO<sub>x</sub> decomposition is negligible at mild temperature, and secondly, *in situ* NO<sub>x</sub> removal *via* adsorption on a solid sorbent is easily achievable. Product molecules adsorbed on microporous materials are protected against plasma induced decomposition in a DBD reactor, as we have demonstrated earlier for the case of ammonia synthesis in a DBD reactor.<sup>19</sup> Plasma cannot develop in sub-micron pores while plasma activated species are too short-lived to diffuse into these pores; therefore adsorbed molecules are protected against plasma-decomposition.<sup>8</sup> Suppressing NO<sub>x</sub> decomposition is expected to improve both energy efficiency and the single pass conversion in a DBD

<sup>a</sup> *Catalytic Processes & Materials, MESA+ Institute for Nanotechnology, University of Twente, P.O. Box 217, 7500 AE Enschede, The Netherlands.*  
E-mail: l.lefferts@utwente.nl

<sup>b</sup> *Ammonia Energy Association, 77 Sands Street, 6th Floor, Brooklyn, NY 11201, USA*

<sup>c</sup> *Koolen Industries, Europalaan 202, 7559 SC Hengelo, The Netherlands*

† Electronic supplementary information (ESI) available: Experimental procedures, including materials and preparation, material characterization, plasma characterization, NO<sub>x</sub> synthesis and adsorption experiments. Results & discussion, including material characterization, plasma characterization, thermal NO<sub>x</sub> TPD study with MgO, and energy cost for MgO regeneration. See DOI: <https://doi.org/10.1039/d3re00593c>



reactor. As earth-alkali metal oxides are known to sorb  $\text{NO}_x$ ,<sup>20</sup> we have selected MgO to demonstrate this concept. We will show that both energy efficiency as well as  $\text{NO}_x$  concentrations in the product stream are drastically improved.

High surface area MgO ( $294 \text{ m}^2 \text{ g}^{-1}$ ) with a particle size between 250 and 300  $\mu\text{m}$  was prepared and characterized as described in ESI† section S1. The experiments were performed using a packed bed DBD reactor with MgO particles, and the  $\text{NO}_x$  concentration was determined with a mass spectrometer (MS), as described in detail in section S2.1.†

Fig. 1 shows the  $\text{NO}_x$  concentration in the outlet as a function of time on igniting the plasma, operating with an  $\text{O}_2$ : $\text{N}_2$  ratio of 1:1, flow rate of  $20 \text{ mL min}^{-1}$ , plasma power of 6.4 W, implying a SEI (specific energy input) of  $19.2 \text{ kJ L}^{-1}$ . The corresponding Lissajous plot is shown in Fig. S3 (see ESI†). It is observed that the  $\text{NO}_x$  outlet concentration is about 0.1 mol% during the first 4 min and increases to about 0.5 mol% afterwards. The change in  $\text{NO}_x$  outlet concentration with time in Fig. 1 is attributed to adsorption of  $\text{NO}_x$  on the MgO sorbent, followed by breakthrough of the  $\text{NO}_x$  in the outlet.

The result shown in Fig. 2 confirms that  $\text{NO}_x$  is indeed adsorbed *in situ*. After exposure to the plasma, the reactor was heated ( $25 \text{ }^\circ\text{C min}^{-1}$ ) in  $\text{N}_2$  ( $10 \text{ mL min}^{-1}$ ), inducing desorption of  $\text{NO}_x$  in absence of plasma. The concentration of  $\text{NO}_2$  is much higher than NO, but we cannot rule out NO formation, as explained in ESI 3.3.† The  $\text{NO}_x$  concentration during desorption is up to 4%, one order of magnitude higher than the  $\text{NO}_x$  concentration during steady-state plasma operation. The amount adsorbed  $\text{NO}_x$  is 0.05 mol per mol MgO.

Fig. 3 compares the TPD (temperature programmed desorption) result after  $\text{NO}_x$  synthesis by plasma illumination during different times with TPD after adsorption of  $\text{NO}_2$  at room temperature. The amount of  $\text{NO}_x$  formed during the plasma experiment obviously varies with plasma time. Fig. 4 shows that the amount of  $\text{NO}_x$  detected with TPD is already

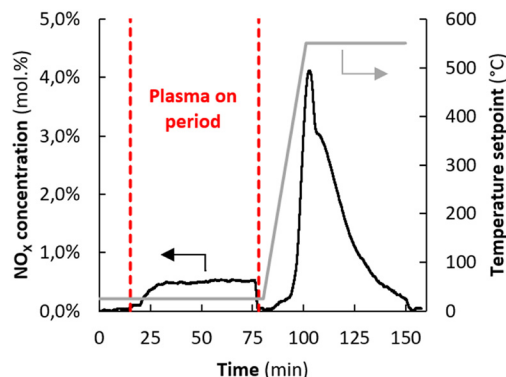


Fig. 2 Typical result of plasma-based  $\text{NO}_x$  synthesis with *in situ* adsorption. Reactor temperature (left axis) and outlet  $\text{NO}_x$  MS signal (right axis) as a function of time. Oven temperature set point during plasma,  $25 \text{ }^\circ\text{C}$ ; total flow rate,  $20 \text{ mL min}^{-1}$ ;  $\text{O}_2$ : $\text{N}_2 = 1:1$ ; plasma power, 6.4 W (SEI =  $19.2 \text{ kJ L}^{-1}$ ); MgO loading, 300 mg (250–300  $\mu\text{m}$ ); plasma duration, 63 min; heating rate after plasma-based  $\text{NO}_x$  synthesis,  $25 \text{ }^\circ\text{C min}^{-1}$ ; pure  $\text{N}_2$ ,  $10 \text{ mL min}^{-1}$ . Samples are thermally pre-treated at  $550 \text{ }^\circ\text{C}$  in  $\text{N}_2$ .

saturated after typically 5 minutes of plasma exposure. The amount is slightly lower than after thermal  $\text{NO}_2$  adsorption in absence of plasma ( $0.055 \text{ mol-NO}_2$  per mol-MgO), in the same order of magnitude as reported by Duong *et al.*<sup>21</sup> for MgO with a slightly lower surface area of  $126 \text{ m}^2 \text{ g}^{-1}$ . The lower amount observed during  $\text{NO}_x$  synthesis with plasma is likely attributed to mild heating induced by the plasma, causing weakly adsorbed  $\text{NO}_2$  to desorb. A similar effect was previously reported for *in situ*  $\text{NH}_3$  removal by a zeolite for plasma-based  $\text{NH}_3$  synthesis.<sup>19</sup> The effective  $\text{NH}_3$  capacity on zeolite 4A decreased by 60% due to heating effects.<sup>19</sup>

The significance of the *in situ* adsorption of  $\text{NO}_x$  from the plasma zone is evident from the reduction in energy consumption *versus* steady-state operation. Steady-state  $\text{NO}_x$  synthesis in this work results in an energy consumption of 93 MJ per mol  $\text{NO}_x$ , in line with literature values reported in the

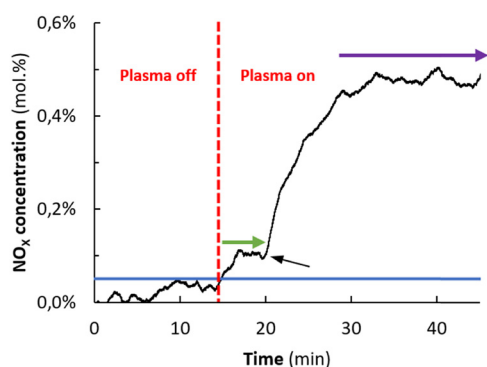


Fig. 1 Outlet  $\text{NO}_x$  concentration as a function of the plasma duration. Oven temperature set point,  $25 \text{ }^\circ\text{C}$ ; total flow rate,  $20 \text{ mL min}^{-1}$ ;  $\text{O}_2$ : $\text{N}_2 = 1:1$ ; plasma power, 6.4 W (SEI =  $19.2 \text{ kJ L}^{-1}$ ); MgO loading, 300 mg (250–300  $\mu\text{m}$ ). The blue line represents the MS sensitivity limit. The green arrow line indicates *in situ*  $\text{NO}_x$  removal with MgO. The black arrow indicates breakthrough of  $\text{NO}_x$  due to sorbent saturation. The purple arrow indicates steady-state operation.

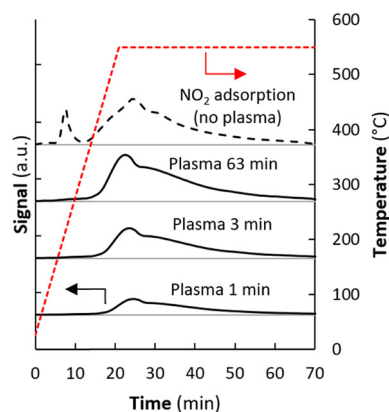


Fig. 3 TPD curve results after plasma-based  $\text{NO}_x$  synthesis ( $\text{O}_2$ : $\text{N}_2 = 1:1$ , plasma duration varied: 1 min, 3 min & 63 min), flow rate  $20 \text{ mL min}^{-1}$  compared to TPD curve after adsorption of  $\text{NO}_2$  at room temperature (2 vol%  $\text{NO}_2$  in 10 vol%  $\text{O}_2$  and 88 vol%  $\text{N}_2$  balance gas during adsorption). TPD in pure  $\text{N}_2$ ,  $10 \text{ mL min}^{-1}$  and heating rate  $25 \text{ }^\circ\text{C min}^{-1}$ .



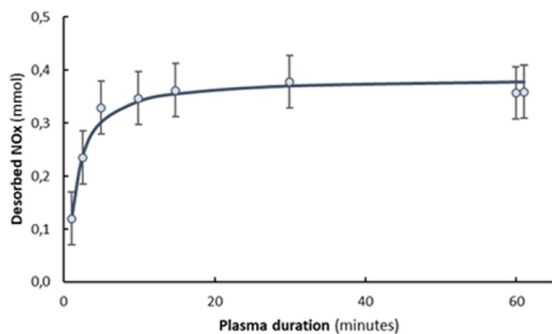


Fig. 4 The effect of plasma duration for plasma-based  $\text{NO}_x$  synthesis with *in situ* adsorption on the amount of adsorbed  $\text{NO}_x$  on 300 mg  $\text{MgO}$ .

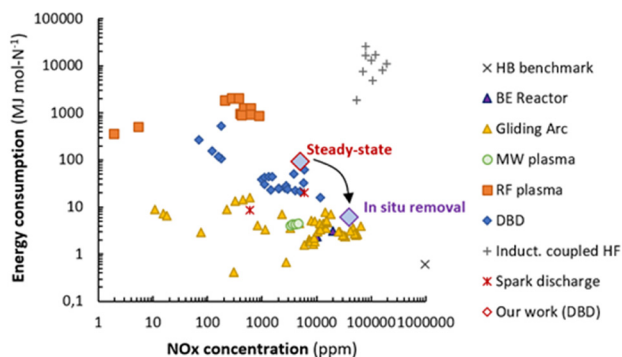


Fig. 5 Comparison of energy consumption for  $\text{NO}_x$  production in various plasma reactors. Original figure reproduced from ref. 6, and data from this work added. Steady-state: red lined diamond. *In situ* removal: purple lined diamond.

range 16–540 MJ per mol  $\text{NO}_x$  for DBD reactors.<sup>13,15–18</sup> In case of *in situ* product removal during 5 minutes, the energy consumption for the plasma reactor and  $\text{NO}_x$  product desorption decreases to 6.0 MJ per mol  $\text{NO}_x$  as calculated in section S3.2† including the energy cost of the desorption step. Effectively, the energy consumption efficiency is improved by a factor 15. As shown in Fig. 5, *in situ* adsorption of  $\text{NO}_x$  in a DBD reactor results in the best performance for a non-thermal plasma-reactor, by both decreasing the energy consumption as well as increasing the  $\text{NO}_x$  concentration in the product stream. Importantly, the  $\text{NO}_x$  concentration raised well above 1%, which is considered as the minimum concentration required for nitric acid production by adsorption in water in a commercially viable process.<sup>22</sup>

Concluding, this work demonstrates that low temperature DBD plasma reactors can produce  $\text{NO}_x$  with similar low energy consumptions obtained with warm plasma reactors like gliding arc reactors and microwave reactors (Fig. 5), by integrating plasma conversion and product separation. Also, the  $\text{NO}_x$  concentration in the product stream is significantly increased. This study demonstrates the concept, but optimization of the (earth-) alkali material as well of the morphology of the adsorbent is likely to result in further improvement.<sup>20</sup> Furthermore, addition of a catalyst,<sup>23</sup> optimization of the dielectric

properties of the adsorbent,<sup>18</sup> and optimization of the plasma properties could be considered.<sup>24,25</sup>

*In situ* product removal is relevant for the wider scientific community working on plasma(-catalytic) conversion. We demonstrate that a significant improvement for  $\text{NO}_x$  synthesis and it is likely that the concept would also applicable for plasma-based  $\text{CO}_2$  dissociation and  $\text{CH}_4$  conversion.<sup>26</sup>

## Conflicts of interest

There are no conflicts to declare.

## Acknowledgements

This project is co-financed by TKI-Energie from Toeslag voor Topconsortia voor Kennis en Innovatie (TKI) from the Ministry of Economic Affairs and Climate Policy, The Netherlands. The authors acknowledge B. Geerdink for technical support, K. Altena-Schildkamp for  $\text{N}_2$  chemisorption experiments and T. Lubbers for XRF analysis. The authors acknowledge K. Van't Veer and A. M. B. Bogaerts from the University of Antwerp for discussions regarding plasma activation of  $\text{N}_2$  in DBD reactors.

## Notes and references

- 1 K. Birkeland, *Trans. Faraday Soc.*, 1906, 2, 98–116.
- 2 S. Eyde, *J. Ind. Eng. Chem.*, 1912, 4, 771–774.
- 3 A. S. Travis, *Nitrogen Capture: The Growth of an International Industry (1900–1940)*, Springer International Publishing, 2018.
- 4 K. H. R. Rouwenhorst, A. S. Travis and L. Lefferts, *Sustainable Chem.*, 2022, 3, 149–171.
- 5 B. S. Patil, Q. Wang, V. Hessel and J. Lang, *Catal. Today*, 2015, 256, 49–66.
- 6 K. H. R. Rouwenhorst, F. Jardali, A. Bogaerts and L. Lefferts, *Energy Environ. Sci.*, 2021, 14, 2520–2534.
- 7 N. Cherkasov, A. O. Ibadon and P. Fitzpatrick, *Chem. Eng. Process.*, 2015, 90, 24–33.
- 8 A. Bogaerts, X. Tu, J. C. Whitehead, G. Centi, L. Lefferts, O. Guaitella, F. Azolina-Jury, H.-H. Kim, A. B. Murphy, W. F. Schneider, T. Nozaki, J. C. Hicks, A. Rousseau, F. Thevenet, A. Khacef and M. Carreon, *J. Phys. D: Appl. Phys.*, 2020, 53, 1–51.
- 9 K. H. R. Rouwenhorst, F. Jardali, A. Bogaerts and L. Lefferts, *Energy Environ. Sci.*, 2023, 16, 6170–6173.
- 10 A. Bogaerts and E. C. Neyts, *ACS Energy Lett.*, 2018, 3, 1013–1027.
- 11 E. Vervloessem, Y. Gorbanev, A. Nikiforov, N. De Geyter and A. Bogaerts, *Green Chem.*, 2022, 24, 916–929.
- 12 W. A. Dekker, E. Snoeck and H. Kramers, *Chem. Eng. Sci.*, 1959, 11, 61–71.
- 13 X. Pei, D. Gidon, Y. J. Yang, Z. Xiong and D. B. Graves, *Chem. Eng. J.*, 2019, 362, 217–228.
- 14 U. Kogelschatz, *Plasma Chem. Plasma Process.*, 2003, 23, 1–46.



- 15 B. S. Patil, N. Cherkasov, J. Lang, A. O. Ibadon, V. Hessel and Q. Wang, *Appl. Catal., B*, 2016, **194**, 123–133.
- 16 Q. Sun, A. Zhu, X. Yang, J. Niu and Y. Xu, *Chem. Commun.*, 2003, 1418–1419.
- 17 A. A. Abdelaziz and H.-H. Kim, *J. Phys. D: Appl. Phys.*, 2020, **53**, 114001–114018.
- 18 Y. Ma, Y. Wang, J. Harding and X. Tu, *Plasma Sources Sci. Technol.*, 2021, **30**, 105002–105013.
- 19 K. H. R. Rouwenhorst, S. Mani and L. Lefferts, *ACS Sustainable Chem. Eng.*, 2022, **10**, 1994–2000.
- 20 C. Verrier, J. H. Kwak, D. H. Kim, C. H. F. Peden and J. Szanyi, *Catal. Today*, 2008, **136**, 121–127.
- 21 T. H. Y. Duong, T. N. Nguyen, H. T. Oanh, T. A. Dang Thi, L. N. T. Giang, H. T. Phuong, N. T. Anh, B. M. Nguyen, V. T. Quang, G. T. Le and T. Van Nguyen, *J. Chem.*, 2019, **2019**, DOI: [10.1155/2019/4376429](https://doi.org/10.1155/2019/4376429).
- 22 K. H. R. Rouwenhorst and L. Lefferts, *Catalysts*, 2020, **10**(9), DOI: [10.3390/catal10090999](https://doi.org/10.3390/catal10090999).
- 23 A. ul R. Salman, B. C. Enger, X. Auvray, R. Lødeng, M. Menon, D. Waller and M. Rønning, *Appl. Catal., A*, 2018, **564**, 142–146.
- 24 H.-H. Kim, Y. Teramoto, A. Ogata, H. Takagi and T. Nanba, *Plasma Processes Polym.*, 2017, **14**, 1–9.
- 25 P. Peng, P. Chen, M. Addy, Y. Cheng, E. Anderson, N. Zhou, C. Schiappacasse, Y. Zhang, D. Chen, R. Hatzenbeller and Y. Liu, *ACS Sustainable Chem. Eng.*, 2019, **7**, 100–104.
- 26 K. H. R. Rouwenhorst and L. Lefferts, *Plasma Processes Polym.*, 2023, 1–8.

